Miscible Blends of Styrene–Acrylic Acid Copolymers with Aliphatic, Crystalline Polyamides

J. A. KUPHAL,[1,2,*] L. H. SPERLING,[1] and L. M. ROBESON[2]

[1]Department of Chemical Engineering, Department of Materials Science and Engineering, Materials Research Center, Center for Polymer Science and Engineering, Lehigh University, Bethlehem, Pennsylvania 18015 and
[2]Air Products and Chemicals, Inc., 7201 Hamilton Blvd., Allentown, Pennsylvania 18195

SYNOPSIS

Styrene–acrylic acid copolymers exhibit miscibility with various aliphatic, crystalline polyamides (e.g., nylon 6, 11, and 12) at 20% acrylic acid content in the copolymer. At 8% acrylic acid, phase separation is observed with the crystalline polyamides. At 14% acrylic acid, partial miscibility is observed with each polyamide, resulting in the T_g's of the constituents shifted toward the other constituent. The miscibility of the styrene–acrylic acid copolymers (> 14 wt % AA) can be ascribed to hydrogen bonding interactions with the polyamides. Styrene–acrylic acid (20% AA) copolymers are miscible with other nylons with alternating amide orientation along the chain (e.g., nylon 6,6 and nylon 6,9). These samples tend to crosslink upon exposure to temperatures above the polyamide melting point unlike the nylon 6, 11, and 12 blends in which branching may only occur. Nylon 11/styrene–acrylic acid blends were chosen for crystallization rate studies. A melting point depression of nylon 11 occurs with addition of the styrene–acrylic acid (20% AA). The Flory–Huggins interaction parameter from the melting point depression is calculated to be −0.27. The crystallization rate of nylon 11 is significantly reduced with the addition of the miscible SAA copolymers (20% AA). The spherulitic growth rate equation predicts this behavior based on a T_g increase with SAA addition.

INTRODUCTION

Miscible blends of structurally different polymers have received considerable interest in the past several decades, offering property profiles of both academic and industrial interest. The earlier studies of miscibility in polymer blends revealed that miscibility was quite unexpected, and only a few miscible systems were observed among the vast number of systems investigated (generally by random choice of the blend constituents).[1-3] More recent reviews revealed an increasing number of miscible pairs of polymeric mixtures.[4-7] It is now recognized that while miscibility is definitely the exception rather than the rule, judicial choice of the constituents can yield miscible blends if simple concepts of specific interactions are properly applied.[8,9] Examples that illustrate the importance of specific interactions in achieving miscibility in polymer blends include hydrogen bonding interactions in poly(ϵ-caprolactone)–poly(vinyl chloride),[10,11] poly(ethylene oxide)–poly(acrylic acid),[12] poly(ethylene oxide)–poly(hydroxy ether) of Bisphenol A,[13] ethylene–ethyl acrylate–carbon monoxide/poly(vinyl chloride),[14] and ethylene–*N*,*N* dimethylacrylamide/poly(vinyl chloride)[15] blends. Other specific interactions noted to yield miscibility in polymer systems include acid–base interactions [e.g., sodium polystyrene sulfonate–poly(vinyl benzyl trimethylammonium chloride)[16]], polar interactions [e.g., poly(vinylidene fluoride)–poly(acrylates)[17] and poly(vinylidene fluoride)–poly(vinyl acetate)[18]], and charge transfer interactions.[19,20] Specific rejection has been recently proposed as another method for achieving miscibility in polymer blends for a blend of a copolymer of units A and B with homopolymer comprised of units C.[21,22] Miscibility is observed when the interaction of A–B is more unfa-

* To whom all correspondence should be addressed.

Journal of Applied Polymer Science, Vol. 42, 1525–1535 (1991)
 CCC 0021-8995/91/061525-11$04.00

vorable than the interactions of A–C and B–C, even when all individual interactions have positive values of the interaction energy density (B) or the Flory–Huggins interaction parameter (χ).

The miscibility of crystalline polyamides with other polymers has been rarely noted in the technical literature relative to other polymer families. This is somewhat surprising as polyamides offer the potential of specific interactions via hydrogen bonding. Ethylene–acrylic acid (EAA) graft copolymers with nylon 6 were noted to exhibit miscibility, and simple blends of EAA copolymers with nylon 6 exhibited a single, broad T_g as noted by Matzner et al.[23] Blends of amorphous polyamides (e.g., Trogamid T, Zytel 330, Bexloy APC-803) with crystalline aliphatic polyamides were investigated by Ellis.[24] It was found that a window of miscibility existed at intermediate levels of methylene unit volume fraction for the crystalline aliphatic polyamides. Poly(ethyl oxazoline) (a tertiary amide polymer) has been noted to be miscible with styrene–acrylonitrile copolymers,[25,26] styrene–acrylic acid copolymers,[25] poly(hydroxy ether) of Bisphenol A,[25] and Trogamid T.[27] Hydrogen bonding interactions of poly(ethyl oxazoline) and ethylene–methacrylic acid copolymer miscible blends were studied by Lichkus et al.[28] Ethylene–N,N-dimethylacrylamide copolymers exhibited miscibility with poly(vinyl chloride) in a specific range of N,N-dimethylacrylamide concentration.[29] Miscibility of nylon 6 blends with poly(acrylic acid) was noted by Jin and Huang,[30] illustrating a significant potential of hydrogen bonding interactions. Lin et al.[31] observed miscibility of poly(ethyl oxazoline) with poly(vinyl phenol) and low molecular weight novolacs (from phenol and formaldehyde condensates).

Ethylene–(meth)acrylic acid copolymer blends with crystalline, aliphatic polyamides have been noted in a number of patent citations[32–37] offering a combination of excellent properties for various application possibilities. Styrene–acrylic acid copolymer blends with nylon 6 have been noted in several patent citations.[38,39] The phase behavior of styrene–acrylic acid copolymers with crystalline alliphatic polyamides (e.g., nylon 6, 11, and 12), however, does not appear in the technical literature to our knowledge. The investigation of the phase behavior of styrene–acrylic acid copolymer blends with crystalline, aliphatic polyamides thus appears warranted, and indeed, the results of this article clearly demonstrate interesting observations as miscibility is observed above a critical level of acrylic acid concentration in the blends with crystalline, aliphatic polyamides.

EXPERIMENTAL

The nylon 11, nylon 12, nylon 6,6, and nylon 6,9 utilized in this study were obtained from Scientific Polymer Products. Nylon 6 was obtained from Allied Chemical under the designation Capron 8200-HS. The styrene–acrylic acid copolymers were prepared via bulk polymerization with pertinent molecular weight data provided in Table I. Weight-averaged molecular weights were determined on a Waters 150C GPC at 35°C. Tetrahydrofuran was used as the mobile phase at a flow rate of 1.0 mL/min. A nonuniversal calibration relative to the retention times of narrow distribution polystyrene standards was employed. Melt flow data were obtained using a Tinius-Olsen melt indexer similar to a procedure described in ASTM D-1238. Melt flow values in Table I were determined after 10-min (MF10) and 30-min (MF30) preheat times at conditions of 200°C and 44 psi. Glass transition temperatures (T_g) were obtained on a Perkin-Elmer DSC-2C at a heating rate of 10°C/min. The T_g data listed in Table I correspond to the midpoint values obtained from the baseline shift at the transition. Feed ratios given in Table I for the styrene–acrylic acid copolymers were confirmed by nuclear magnetic resonance (NMR) analysis.

Melt blends of nylon 11 and 12 with the styrene–acrylic acid copolymers were prepared in a Brabender melt mixer at 200°C, and blends involving nylon 6 were prepared at 230°C. Melt blends involving nylon 6,6 and nylon 6,9 were prepared in a brabender at 265 and 220°C, respectively. Samples were subsequently compression molded into 20- and 40-mil plaques for further characterization. Dynamic mechanical spectroscopy (DMS) was performed on a Rheometrics RMS-605 mechanical spectrometer at a frequency of 1 Hz. Samples for both DSC and DMS measurements were stored under vacuum or in a dessicator for at least 24 h prior to testing. Designation of composition for the copolymers and blends discussed in this article are by weight percentages.

Table I Characterization Data for Styrene–Acrylic Acid Copolymers

Styrene–Acrylic Acid Feed Ratio (by wt)	M_w	T_g (°C)	MF10 (dg/min)	MF30 (dg/min)
92 : 8	86,000	125	6.7	7.3
86 : 14	83,000	137	2.9	3.0
80 : 20	71,000	142	5.0	5.0

Isothermal crystallization studies were performed on a Perkin-Elmer DSC-2C using an isopropanol–dry ice mixture to maintain a constant cold source at approximately −50°C. If a constant-temperature source was not maintained from sample to sample, considerable variations in experimental data occurred (e.g., the value of the time to maximum crystallization rate, $t_{c,max}$). Approximately 15 mg of nylon 11 or a nylon 11–SAA blend was enclosed in a DSC aluminum pan/lid and placed in the sample side of the cell block. An equal weight of aluminum was placed in the reference side to counteract heat transfer differences upon rapid cooling. This was to provide thermal equilibrium in a shorter period of time. Once the cell was loaded, the temperature was elevated to 210°C and maintained for 3 min to ensure sufficient time to adequately melt all of the sample. It should be noted that a temperature of 210°C was chosen to provide thorough melting while not degrading the sample under investigation. Note that this temperature is above the equilibrium melting point for both nylon 11 and the nylon 11–SAA blends. After the 3-min preheat, the sample was rapidly cooled at a rate of 320°C/min to the isothermal crystallization temperature (T_c) chosen. The resultant exotherm was analyzed to determine the heat of crystallization (ΔH_c), time to maximum crystallization rate ($t_{c,max}$), and the time to full crystallization ($t_{c,\infty}$).

Experimental values for the time to maximum crystallization rate ($t_{c,max}$) were determined as the time required to obtain the maximum peak in the exotherm. This value was corrected by subtracting the time to arrive at the isothermal temperature from the melt, for example, roughly 25 s were required to lower the DSC cell temperature from 210 to 160°C. This correction factor was consistent throughout the analysis and of course varied depending on the isothermal temperature chosen. The consistency of the correction factor was an important indication of how constant the cold source reservoir was maintained to provide the driving force required to obtain reproducible $t_{c,max}$ values. Isothermal temperatures were chosen for Avrami analysis where a sufficient baseline could be established prior to the onset of crystallization. Other $t_{c,max}$ values obtained where crystallization had begun prior to establishing a baseline were included in the figures and appeared reasonable based on the curve fitting techniques employed.

Melting point data was obtained on both nylon 11 and nylon 11–SAA blends in order to determine the equilibrium melting points according to the Hoffman–Weeks theory.[40] In order to develop a consistent technique in obtaining these data, the following procedure was established. Once the time to full crystallinity was reached (as described above), each sample received an additional 1 h at the designated isothermal temperature. At this point, the sample was heated at a rate of 10°C/min from the isothermal temperature to a point at which the melting endotherm was completed. The maximum peak in the endotherm represented the melting temperature for the sample previously held at a given isothermal temperature. Several temperatures were employed to obtain data points in order to extrapolate to the $T'_m = T_c$ line, which yields the Hoffman–Weeks equilibrium melting point for each sample.

EXPERIMENTAL RESULTS

The acrylic acid content of the styrene–acrylic acid (SAA) copolymers used in this investigation was critical in obtaining varying degrees of miscibility with nylon 6, 11, and 12, as illustrated in Figures 1–6. All the samples based on the SAA (8% AA) were phase separated. The blends based on SAA (14% AA) exhibited partial miscibility with each of the crystalline, aliphatic polyamides (nylon 6, 11, and 12). The blends based on SAA (20% AA) exhibited miscibility with all of these polyamides. The blends based on SAA (14% AA) exhibit two glass transition temperatures intermediate between the unblended constituent values, thus exhibiting partial miscibility resulting from the presence of a polyamide rich

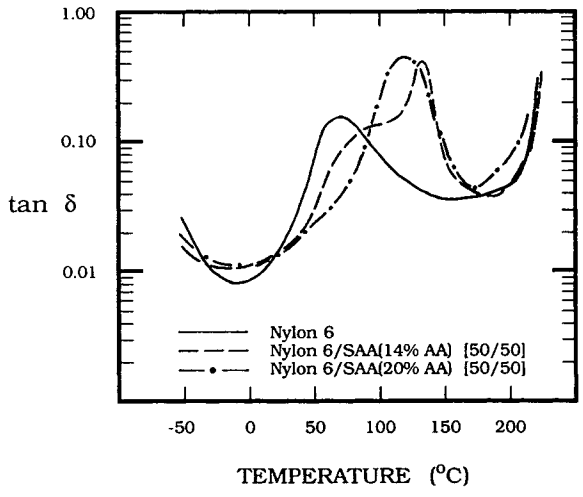

Figure 1 Mechanical loss (tan δ) vs. temperature for nylon 6–SAA blends obtained on Rheometrics RMS-605 mechanical spectrometer (frequency 1 Hz): (—) nylon 6, (---) nylon 6–SAA (14% AA) (50 : 50), and (— ● —) nylon 6–SAA (20% AA) (50 : 50).

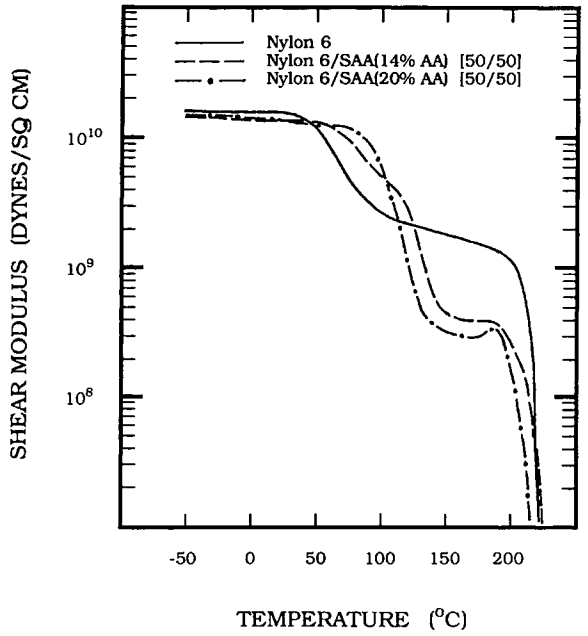

Figure 2 Shear modulus (G') vs. temperature for nylon 6–SAA blends obtained on Rheometrics RMS-605 mechanical spectrometer (frequency 1 Hz); (—) nylon 6, (---) nylon 6–SAA (14% AA) (50 : 50), and (— ● —) nylon 6–SAA (20% AA) (50 : 50).

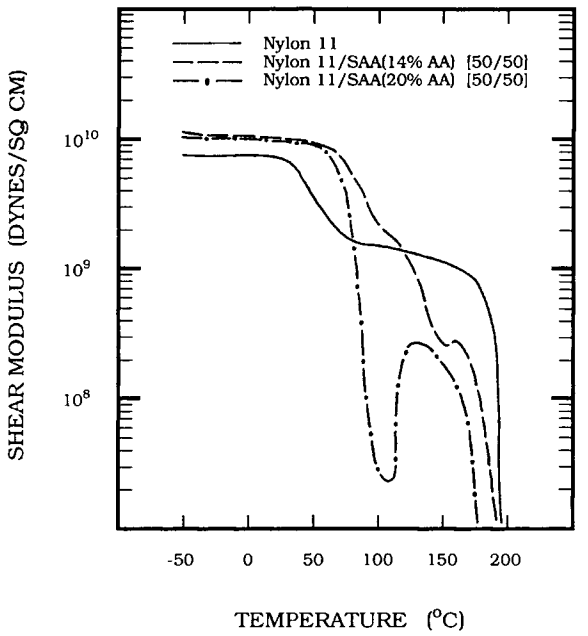

Figure 4 Shear modulus (G') vs. temperature for nylon 11–SAA blends obtained on Rheometrics RMS-605 mechanical spectrometer (frequency 1 Hz): (—) nylon 11, (---) nylon 11–SAA (14% AA) (50 : 50), and (— ● —) nylon 11–SAA (20% AA) (50 : 50).

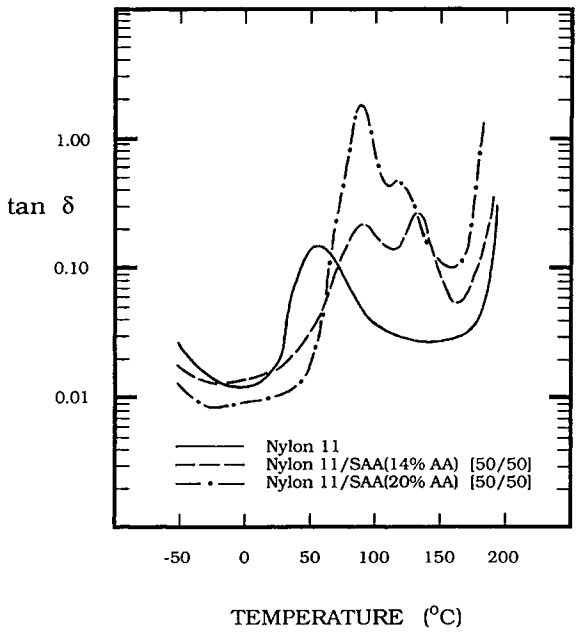

Figure 3 Mechanical loss (tan δ) vs. temperature for nylon 11–SAA blends obtained on Rheometrics RMS-605 mechanical spectrometer (frequency 1 Hz): (—) nylon 11, (---) nylon 11–SAA(14% AA) (50 : 50), and (— ● —) nylon 11–SAA (20% AA) (50 : 50).

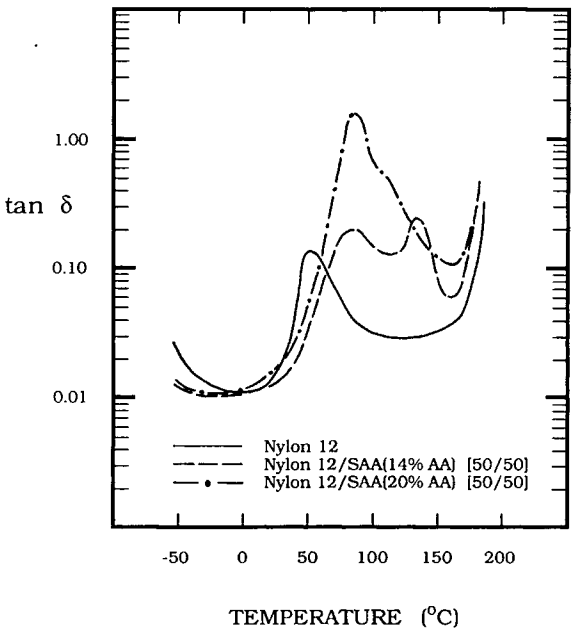

Figure 5 Mechanical loss (tan δ) vs. temperature for nylon 12–SAA blends obtained on Rheometrics RMS-605 mechanical spectrometer (frequency 1 Hz): (—) nylon 12, (---) nylon 12–SAA (14% AA) (50 : 50), and (— ● —) nylon 12–SAA (20% AA) (50 : 50).

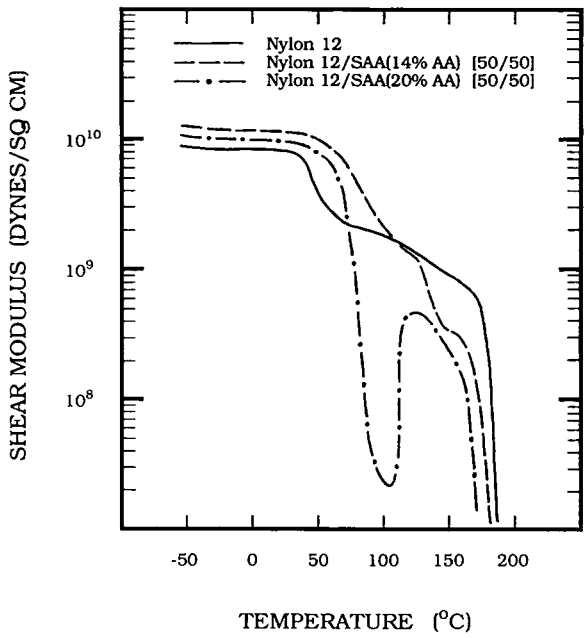

Figure 6 Shear modulus (G') vs. temperature for nylon 12–SAA blends obtained on Rheometrics RMS-605 mechanical spectrometer (frequency 1 Hz): (—) nylon 12, (---) nylon 12–SAA (14% AA) (50 : 50), and (— ● —) nylon 12–SAA (20% AA) (50 : 50).

phase and a styrene–acrylic acid rich phase. With the SAA (20% AA) blends, however, single, sharp glass transition temperatures are observed illustrating single-phase behavior. The modulus-temperature curves reflect the differences in miscibility behavior as the SAA (14% AA) blends are crystalline as molded whereas the 20 wt % AA based SAA blends crystallize during the temperature excursion of the DMS measurement (see Figs. 2, 4, and 6). This illustrates the much slower crystallization rate of the miscible blends based on SAA (20 wt % AA). This is expected due to the increase in the glass transition temperature of the blend over that of the nylon homopolymer. The result is inhibition of the crystallization rate of the aliphatic, crystalline polyamides. This is predicted by the spherulitic growth rate equation where the glass transition temperature is an important variable.[41]

Calorimetry data were obtained on the polyamides and their respective blends with styrene–acrylic acid copolymers (at 14 and 20% AA). The samples (as compression molded) were heated at 10°C/min to determine the heat of crystallization (ΔH_c), heat of fusion (ΔH_f), and melting temperature (T_m). After which, they were cooled at 10°C/min to determine ΔH_c and T_c and then reheated at 10°C/min to determine ΔH_c, ΔH_f, and T_m. The results are tabulated in Table II.

The crystallization kinetics of the blends were analyzed according to the Avrami equation[42] in the form of

$$X/X^{\infty} = 1 - \exp(-Kt^n) \qquad (1)$$

where t is the time at a specific temperature T with $X = 0$ at $t = 0$ (X is the degree of crystallinity at time t) and X^{∞} is the ultimate degree of crystallinity; K and n are constants utilized to fit the experimental results. The X/X^{∞} data were determined from integration of the area under the crystallization exotherm of the isothermal DSC trace. The plot of

Table II Calorimetry Data on Polyamide/SAA Blends

	Heating (10°C/min)			Cooling (10°C/min)		Reheating (10°C/min)		
	ΔH_c (cal/g)	ΔH_f (cal/g)	T_m (°C)	ΔH_c (cal/g)	T_c (°C)	ΔH_c (cal/g)	ΔH_f (cal/g)	T_m (°C)
Nylon 6	—	19.8	221	17.4	184	—	17.7	219
Nylon 6/SAA (14% AA) (50/50)	—	7.04	218	8.27	174	—	7.07	218
Nylon 6/SAA (20% AA) (50/50)	1.28	7.27	212	6.60	151	—	6.06	207
Nylon 11	—	14.1	190	12.8	163	—	13.9	190
Nylon 11/SAA (8% AA) (50/50)	—	6.78	189	6.14	161	—	6.92	188
Nylon 11/SAA (14% AA) (50/50)	0.50	6.26	183	8.32	148	0.32	6.20	182
Nylon 11/SAA (20% AA) (50/50)	4.81	6.07	175	0.61	126	4.71	4.77	173
Nylon 12	—	17.7	180	16.1	151	—	18.0	180
Nylon 12/SAA (14% AA) (50/50)	—	6.84	176	8.87	145	—	6.91	175
Nylon 12/SAA (20% AA) (50/50)	6.21	6.41	169	—	—	3.86	4.31	168

$\log_{10}[-\ln(1 - X/X^{\infty})]$ vs. $\log_{10}t$ is shown in Figures 7 and 8 for nylon 11 and a blend of nylon 11 with SAA (20% AA). Linear response for these data were obtained below $X/X^{\infty} = 0.7$.

In order to fit the experimental results for the time to maximum crystallization rate ($t_{c,\max}$) at the specified isothermal crystallization temperature, Eq. (1) was assumed to be of the form

$$X/X^{\infty} = 1 - \exp[-K'(Gt)^n] \qquad (2)$$

The assumption of eq. (2) is based on the value of K′ being a function of the linear growth rate raised to the nth power as established by prior references.[43,44] The spherulitic growth rate in the radial direction, $G = dr/dt$, has been defined by Gornick and Hoffman[45] as

$$G = G_0 \exp\left(-\frac{\Delta F^*}{RT}\right)\exp\left(-\frac{4b_0\sigma\sigma_e T_m^0}{\Delta H_f (T_m^0 - T_c) k T_c}\right) \qquad (3)$$

where ΔF^* is the energy barrier restricting movement to the crystallizing surface as typically defined by the WLF equation[46]:

$$\Delta F^* = \frac{4120 T_c}{51.6 + T_c - T_g} \qquad (4)$$

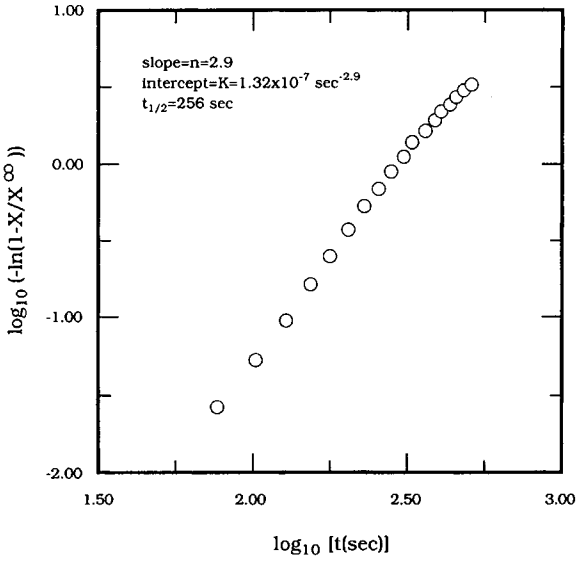

Figure 7 Avrami plot for nylon 11 isothermally crystallized at 173°C.

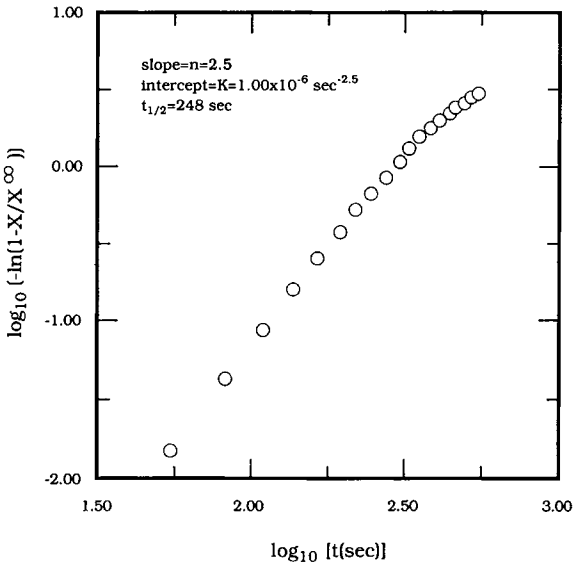

Figure 8 Avrami plot for nylon 11–SAA (20% AA) (50 : 50) isothermally crystallized at 140°C.

and where b_0 = monolayer thickness
σ = lateral interfacial free energy
σ_e = interfacial free energy of chain folded surface
ΔH_f = heat of fusion
T_c = crystallization temperature

The second derivative of Eq. (2) set equal to zero yields the following value of $t_{c,\max}$ (the time to maximum crystallization rate):

$$\left(\frac{n-1}{K'n}\right)^{1/n} = G t_{c,\max} \qquad (5)$$

As an approximation, the form of the rate equation was assumed to be

$$G = A \exp\left(-\frac{B}{51.6 + T_c - T_g}\right)\exp\left(\frac{-CT_m^0}{(T_m^0 - T_c)T_c}\right) \qquad (6)$$

where

$$A = (K')^{1/n} G_0 (1 - X_a)$$

$$B = 4120/R$$

$$C = 4b_0\sigma\sigma_e/\Delta H_f k$$

and $1 - X_a$ is the weight fraction of crystalline component b (this term is added for the blends to

account for the dilution effect of an added miscible noncrystalline component as established by Robeson).[11]

Thus, the equation to fit the crystallization kinetics is

$$\left(\frac{n-1}{n}\right)^{1/n}\frac{1}{t_{c,\max}} = A\exp\left(-\frac{B}{51.6 + T_c - T_g}\right) \times \exp\frac{-CT_m^0}{(T_m^0 - T_c)T_c} \quad (7)$$

In order to obtain the constants for Eq. (7), n (the Avrami constant), T_m^0 (the equilibrium melting temperature), $t_{c,\max}$, and T_g experimental values are required. The T_m^0 data were obtained using the Hoffman–Weeks extrapolation technique[40] as noted previously. The results are illustrated in Figure 9 for nylon 11, nylon 11–SAA (20% AA) (50 : 50 blend), and nylon 11–SAA (20% AA) (75 : 25 blend). Values for n were obtained from Eq. (1) as noted in Figures 7 and 8 for nylon 11 and the nylon 11–SAA (20% AA) (50 : 50) blend), respectively. The values for $t_{c,\max}$ were obtained from the isothermal crystallization exotherm data noted previously. The T_g data were obtained from the DMS data. With these experimental values determined, A, B, and C parameters for Eq. (7) were obtained to provide the best fit according to the procedure. These results are summarized in Table III.

The results of this analysis are illustrated in Figure 10 for nylon 11, nylon 11–SAA (20% AA) (50 : 50 blend), and nylon 11–SAA (20% AA) (75 : 25 blend), where the solid line illustrates the best fit of Eq. (7) to the experimental data. The crystallization rate of nylon 11 was too rapid to experimentally determine the minimum in the data presented in Figure 10. Quenching nylon 11 in liquid nitrogen, ice water, or a dry ice–isopropanol mixture did not allow for an amorphous specimen as complete crystallization occurred during the cooling cycle. Thus values of crystallization times at crystallization temperatures lower than the temperature where the maximum crystallization rate was expected to occur could not be obtained. Quenching of thin (less than 5-mil) nylon 11 films also failed to yield any improvement in the ability to obtain fully amorphous samples. Quenching nylon 11–SAA (20% AA) 50 : 50 blend) and nylon 11–SAA (20% AA) (75 : 25 blend) to an amorphous state appeared possible based on data obtained from DSC analysis where a distinct exotherm was observed upon heating. The lowered crystallization rate of the blends is a consequence of the increased T_g of the crystallizable component which is predicted by the spherulitic growth rate equation.

Significant differences were observed with 50 : 50 blends of nylon 6,6 and nylon 6,9 with styrene–acrylic acid (20% AA) compared to similar blends involving nylon 6, 11, and 12. At the mixing con-

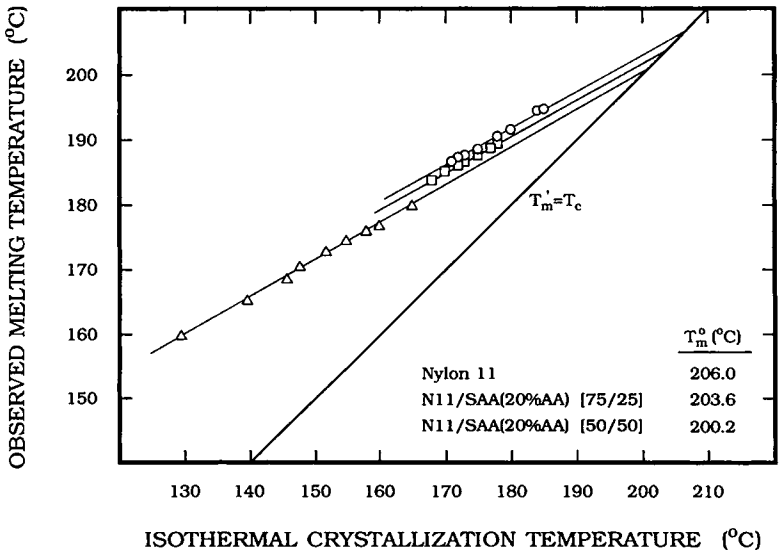

Figure 9 Hoffman–Weeks extrapolation to determine equilibrium melting temperatures for nylon 11 (○), nylon 11–SAA (20% AA) (75 : 25) (□), and nylon 11–SAA (20% AA) (50 : 50) (△).

Table III Experimental Data Used in Equation (7) to Determine Constants *A*, *B*, and *C*

	n	T_g (°C)	T_m^0 (°C)	A (s^{-1})	B (°K)	C (°K)
Nylon 11	2.9	54	206.0	8.37×10^{-11}	−3919	169
Nylon 11–SAA (20% AA) (75 : 25)	2.8	73[a]	203.6	2850	535	338
Nylon 11–SAA (20% AA) (50 : 50)	2.5	90	200.2	1.81×10^{7}	1322	500

[a] Calculated from the Fox equation ($1/T_{g,\text{blend}} = W_1/T_{g1} + W_2/T_{g2}$) in order to obtain a value for a completely amorphous sample.

ditions (~ 265°C) required for nylon 6,6 and SAA, crosslinking occurred simultaneously with mixing of the components. With nylon 6,9 (~ 220°C), mixing was possible but the melt viscosity appeared to increase with mixing time exposure. Melt flow studies listed in Table IV on comparative blends illustrate this observation. Comparative data on a nylon 6–SAA (20% AA) blend indicate increasing melt flow with preheat time.

Calorimetry data obtained on nylon 6,6 and nylon 6,9 blends with SAA (20% AA) are listed in Table V. The results show a significant reduction in the melting point as well as in the crystallization kinetics. In fact, the nylon 6,6–SAA (20% AA) blend was so highly crosslinked that no crystallization was observed after the initial heating cycle. The lowered melting point is due to a combination of the melting point depression due to a miscible additive and the crosslinking that occurred during blending, molding, and the temperature excursion of the calorimetry experiment.

DISCUSSION OF RESULTS

The dynamic mechanical results (Figs. 1–6) demonstrate miscibility of nylon 6, 11, and 12 with styrene–acrylic acid copolymers at 20 wt % acrylic acid in the copolymer. At a lower acrylic acid level (14% AA), only partial miscibility was observed for each blend with nylon 6, 11, and 12 yielding two glass transitions intermediate between the unblended values of the blend constituents. This is the result of a nylon rich phase and a styrene–acrylic acid copolymer rich phase. At lower acrylic acid levels (8% AA) nearly complete phase separation was observed.

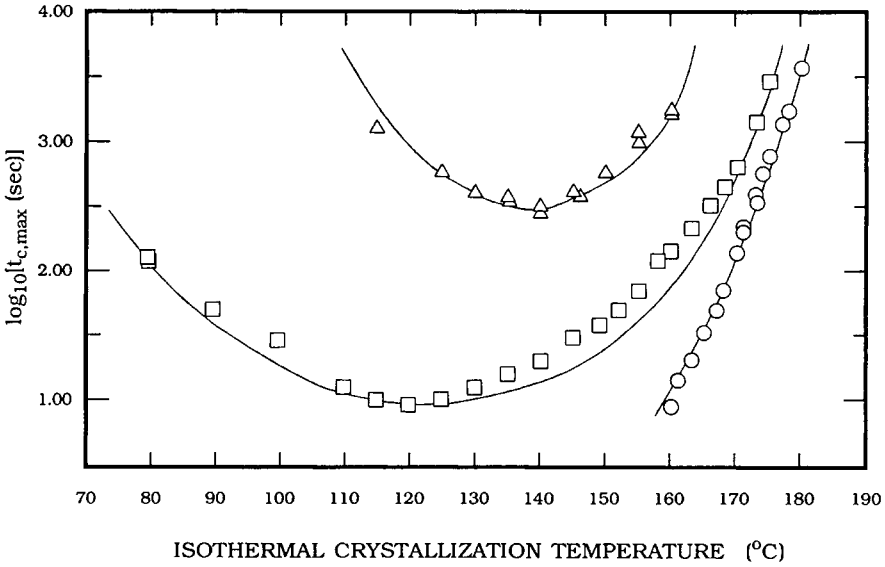

Figure 10 Time to maximum crystallization rate ($t_{c,\max}$) vs. isothermal crystallization temperature (T_c) for nylon 11 (○), nylon 11–SAA (20% AA) (75 : 25) (□), and nylon 11–SAA (20% AA) (50 : 50) (△). Solid line represents curve fitting results using experimental data in Eq. (7).

Table IV Melt Flow Comparison of Nylon 6 and Nylon 6,9 in Blends with Styrene–Acrylic Acid Copolymer (20% AA) at 230°C and 44 psi

	MF10 (dg/min)	MF20 (dg/min)	MF30 (dg/min)
Nylon 6	6.9	6.7	7.0
Nylon 6,9	33	35	31
Nylon 6–SAA (20% AA) (50 : 50)	89	150	160
Nylon 6,9–SAA (20% AA) (50 : 50)	No flow	No flow	No flow

The shear modulus (G')–temperature data (Figs. 2, 4 and 6) demonstrate distinct differences in the behavior of the samples above T_g. The nylon 6, 11, and 12 samples as well as the partially miscible systems based on 50 : 50 blends of these polyamides with SAA (14% AA) exhibit full crystallinity as molded. The polyamide blends with SAA (20% AA), however, exhibit crystallization above T_g as the temperature is increased during the DMS heating excursion. This is a result of the significantly reduced crystallization rate of the blend due to the increase in T_g over the unblended, crystallizable component. This is expected as predicted by the spherulitic growth rate equation.

The equilibrium melting point for nylon 11 was determined to be 206.0°C using the Hoffman–Weeks extrapolation technique. A lower value of the nylon 11 melting point (T_m^0 = 200.2°C) was determined for nylon 11/styrene–acrylic acid (20% AA) 50 : 50 blend. From these values, the Flory–Huggins interaction parameter, χ_{12}, can be calculated from the expression (as noted by Nishi and Wang[47]):

$$\frac{1}{T_{m,b}^0} - \frac{1}{T_m^0} = \frac{-RV_2\chi_{12}}{\Delta H_f^0 V_1}(1 - \phi_2)^2$$

$$\chi_{12} = -0.27 \qquad (8)$$

This demonstrates a reasonable interaction for this blend as expected from the hydrogen bonding capabilities of amide–acid groups.

The heat of fusion and heat of crystallization of the polyamides in the blends with SAA (20% AA) (Table II) appear lower than their weight-corrected values would predict based on the same degree of crystallinity. This is probably due to two factors; a kinetic factor and heat of mixing. The kinetic factor is related to the much faster rate of crystallinity for the unblended polyamides, thus yielding a higher degree of crystallinity within the time scale of the temperature excursion of the experiments noted in Table II. The other factor, though probably small, is that the polyamide crystalline phase mixes with the amorphous polyamide–SAA phase, resulting in an exothermic heat of mixing that lowers the observed heat of fusion (endothermic). The reverse occurs upon crystallization, where the observed heat of crystallization (exothermic) is decreased by the heat of demixing (endothermic).

In order to compare the degree of crystallinity under conditions that reduce the kinetic differences, heat of crystallization and heat of fusion values were obtained under isothermal conditions where the $t_{c,max}$ (time to reach maximum crystallization rate) values were similar for nylon 11 and nylon 11–SAA (20%

Table V Calorimetry Data for Nylon 6,6 and 6,9 and Blends with Styrene–Acrylic Acid (20% AA) Copolymer

	Heating (10°C/min)			Cooling (10°C/min)		Reheating (10°C/min)		
	ΔH_c (cal/g)	ΔH_f (cal/g)	T_m (°C)	ΔH_c (cal/g)	T_c (°C)	ΔH_c (cal/g)	ΔH_f (cal/g)	T_m (°C)
Nylon 6,6	—	17.1	262	16.9	229	—	18.0	262
Nylon 6,9	2.77	13.1	210	12.2	178	2.86	13.0	210
Nylon 6,6–SAA (20% AA) (50 : 50)	—	7.26	248	—	—	—	—	—
Nylon 6,9–SAA (20% AA) (50 : 50)	1.28	4.20	198	5.0	152	0.97	2.96	192

AA) (50 : 50 blend). These data are listed in Table VI and show that the heat of crystallization and heat of fusion for nylon 11 (corrected for weight percent) is higher in the blend than for unblended nylon 11. This higher level of crystallinity (of the crystallizable component) in the blend is not unexpected and has been observed in previous blends containing a crystallizable component.[48-50] This was explained by Harris and Robeson[51,52] as due to increased mobility in the interlamellar regions. This in turn is due to a noncrystallizing diluent as well as the increased volume present (due to the diluent), allowing for a higher level of crystallinity prior to the onset of spherulitic impingement. This can be better understood by noting that the crystallization of polymer from solvent solutions generally yields much higher levels of crystallinity than undiluted melt crystallization. In the case for polymer blends, the "solvent" is a high molecular weight polymer.

The reaction of the acrylic acid of the copolymer with amine end groups of the polyamide is apparent. Additionally, the reaction of the amide group with the acrylic acid is also possible (with water present).

Table VI Isothermal Crystallization Data

T_c (°C)	$t_{c,max}$ (minutes)	ΔH_c (cal/g)	ΔH_f (cal/g)
	Nylon 11		
171	3.40	9.37	10.8
173	5.34	9.28	10.5
175	8.07	9.26	9.85
177	21.69	9.62	—
178	28.04	9.09	9.27
	Nylon 11/SAA (20% AA) (50/50 blend)		
125	9.18	6.40	6.98
130	6.45	6.24	6.05
135	5.61	6.00	6.68
140	4.58	6.40	5.55
145	5.95	6.29	7.11
150	8.32	6.62	—
155	15.41	6.21	7.79
160	28.44	5.32	7.49
	Nylon 11/SAA (20% AA) (75/25 blend)		
166	5.22	8.84	9.84
170	10.42	7.73	9.41
172	20.56	7.80	8.80
173	23.42	7.72	9.07
175	45.16	8.28	8.52

Although the samples were well dried, residual water will be present as well as water from the amine–acid reaction. The nylon 6, 11, and 12 will have only one amine terminal group per molecule whereas the nylon 6,6 and nylon 6,9 can have two terminal amine groups per molecule. The severe level of crosslinking with nylon 6,6 (resulting in a severe reduction in crystallization rate) indicates both amine–acid as well as amide–acid reactions occur. The orientation of the amide groups along the polyamide chain for nylon 6, 11, and 12 (alternating $-\overset{\overset{O}{\|}}{C}-$ and $-\overset{\overset{H}{|}}{N}-$ units) combined with only one terminal amine group will only lead to branching. With nylon 6,6 and nylon 6,9, however, two terminal amine groups are possible along with the chain sequence of $-\overset{\overset{O}{\|}}{C}-\overset{\overset{H}{|}}{N}-$ followed by $-\overset{\overset{H}{|}}{N}-\overset{\overset{O}{\|}}{C}-$ units. Both of these features allow for the potential of crosslinking. Similar crosslinking reactions have been noted for polymers capable of transesterification where crosslinking occurs on extended time–temperature exposure [e.g., poly(hydroxyether) of Bisphenol A with poly(butylene terephthalate)[48] or with polyarylate[53]].

REFERENCES

1. D. J. Buckley, *Trans. N.Y. Acad. Sci.*, **29**(2), 735 (1967).
2. L. Bohn, *Rubber Chem Technol.*, **41**, 495 (1968).
3. J. A. Manson and L. H. Sperling, *Polymer Blends and Composites*, Plenum Press, New York, 1976.
4. S. Krause, *J. Macromol. Sci., Rev. Macromol. Chem.*, **C7**, 251 (1972).
5. S. Krause, in *Polymer Blends*, D. R. Paul and S. Newman, Eds., Academic Press, New York, 1978, chap. 2.
6. O. Olabisi, L. M. Robeson, and M. T. Shaw, in *Polymer–Polymer Miscibility*, Academic Press, New York, 1979, chap. 5.
7. L. A. Utracki, *Polymer Alloys and Blends*, Hauser, Munich, 1989.
8. L. M. Robeson, paper presented at "Workshop on New Polymeric Materials: Advances in Polymeric Alloys and Composites," Leuven, Belgium, Oct. 22, 1986.
9. F. Cangelosi and M. T. Shaw, *Polym. Eng. Sci.*, **23**, 669 (1983).
10. J. V. Koleske and R. D. Lundberg, *J. Polym. Sci., Part A-2*, **7**, 795 (1969).
11. L. M. Robeson, *J. Appl. Polym. Sci.*, **17**, 3607 (1973).

12. K. L. Smith, A. E. Winslow, and D. E. Petersen, *Ind. Eng. Chem.*, **51**, 1361 (1959).
13. L. M. Robeson, W. F. Hale, and C. N. Merriam, *Macromolecules*, **14**, 1644 (1981).
14. L. M. Robeson and J. E. McGrath, *Polym. Eng. Sci.*, **17**, 300 (1977).
15. M. Matzner, L. M. Robeson, E. W. Wise, and J. E. McGrath, *Makromol. Chem.*, **183**, 2871 (1982).
16. A. S. Michaels, *Ind. Eng. Chem.*, **57**(10), 32 (1965).
17. R. E. Bernstein, D. R. Paul, and J. W. Barlow, *Polym. Eng. Sci.*, **18**, 683 (1978).
18. R. E. Bernstein, D. C. Wahrmund, J. W. Barlow, and D. R. Paul, *Polym. Eng. Sci.*, **18**, 1220 (1978).
19. T. Sulzberg and R. J. Cotter, *J. Polym. Sci., Part A-1*, **8**, 2747 (1970).
20. K. Abe, S. Haibara, Y. Itoh, and S. Senoh, *Makromol. Chem.*, **186**, 1505 (1985).
21. R. P. Kambour, J. T. Bendler, and R. C. Bopp, *Macromolecules*, **16**, 753 (1983).
22. D. R. Paul and J. W. Barlow, *Polymer*, **25**, 487 (1984).
23. M. Matzner, D. L. Schober, R. N. Johnson, L. M. Robeson, and J. E. McGrath, in *Permeability of Plastic Films and Coatings*, H. B. Hofenberg, Ed., Plenum, New York, 1975, p. 125.
24. T. S. Ellis, *Macromolecules*, **22**, 742 (1989).
25. K. M. McCreedy, H. Keskkula, J. C. Pawloski, and E. H. Yonkers, U.S. Pat. 4,678,833; assigned to Dow Chemical Co., July 7, 1987.
26. J.-L. G. Pfennig, H. Keskkula, and D. R. Paul, *J. Appl. Polym. Sci.*, **32**, 3657 (1986).
27. L. M. Robeson, in *Contemporary Topics in Polymer Science*, Plenum Press, New York, Vol. 6, p. 177 (1989).
28. A. M. Lichkus, P. C. Painter, and M. M. Coleman, *Macromolecules*, **21**, 2636 (1988).
29. M. Matzner, L. M. Robeson, E. W. Wise, and J. E. McGrath, *Coatings and Plastics Prepr., Am. Chem. Soc., Div. Org. Coatings and Plastics Chem.*, **37**(1), 123 (1977).
30. Y. Jin and R. Y. M. Huang, *J. Appl. Polym. Sci.*, **36**, 1799 (1988).
31. P. Lin, C. Clash, E. M. Pearce, T. K. Kwei, and M. A. Aponte, *J. Polym. Sci., Part B: Polym. Phys.*, **26**, 603 (1988).
32. R. V. Meyer and P. Tacke, U.S. Pat. 4,246,371; assigned to Bayer, Jan. 20, 1981.
33. H. W. Starkweather, Jr., U.S. Pat. 3,492,367; assigned to E. I. duPont de Nemours and Co., Jan. 27, 1970.
34. P. W. Flood, C. D. Mason, and S. R. Schulze, U.S. Pat. 4,335,223; assigned to Allied Corp., June 15, 1982.
35. S. M. Aharoni and T. Largman, U.S. Pat. 4,417,031; assigned to Allied Corp., Nov. 22, 1983.
36. G. M. Lancaster and S. M. Hoenig, U.S. Pat. 4,532,100; assigned to Dow Chemical Co., July 30, 1985.
37. R. V. Meyer, R. Dhein, and F. Fahnler, U.S. Pat. 4,321,336; assigned to Bayer, March 23, 1982.
38. M. Motai and S. Kimura, Jpn. Kokai Tokkyo Koho JP 62, 185, 724 [87,185,724]; assigned to Japan Synthetic Rubber Co., Ltd., Aug. 14, 1987.
39. Jpn. Kokai Tokkyo Koho 81 62,844; assigned to Asahi-Dow Ltd., May 29, 1981.
40. J. D. Hoffman and J. J. Weeks, *J. Chem. Phys.*, **37**, 1723 (1962).
41. J. D. Hoffman and J. I. Lauritzen, Jr., *J. Research-Nat. Bureau Standards-A Phys. and Chem.*, **65A**(4), 297 (1961).
42. M. Avrami, *J. Chem. Phys.*, **8**, 212 (1940).
43. L. Mandelkern, *Polymer*, **5**, 637 (1964).
44. B. Wunderlich, *Macromolecular Physics, Vol. 2: Crystal Nucleation, Growth, Annealing*, Academic Press, New York, 1976, chap. 6.
45. F. Gornich and J. D. Hoffman, in *Nucleation Phenomena*, A. S. Michaels, Ed., Am. Chem. Soc., Washington, D.C., 1966, p. 53.
46. M. L. Williams, R. F. Landel, and J. D. Ferry, *J. Am. Chem. Soc.*, **77**, 3701 (1955).
47. T. Nishi and T. T. Wang, *Macromolecules*, **8**, 909 (1975).
48. L. M. Robeson and A. B. Furtek, *J. Appl. Polym. Sci.*, **23**, 645 (1979).
49. D. Allard and R. E. Prudhomme, *J. Appl. Polym. Sci.*, **27**, 559 (1982).
50. R. N. Mohn, D. R. Paul, J. W. Barlow and C. A. Cruz, *J. Appl. Polym. Sci.*, **23**, 575 (1979).
51. J. E. Harris and L. M. Robeson, *J. Polym. Sci., Part B: Polym. Phys., Ed.*, **25**, 311 (1987).
52. J. E. Harris and L. M. Robeson, *J. Appl. Polym. Sci.*, **35**, 1877 (1988).
53. L. M. Robeson, *J. Appl. Polym. Sci.*, **30**, 4081 (1985).

Received May 11, 1990
Accepted July 9, 1990